International Journal of Advanced Engineering Application (IJAEA)
Volume 3 Issue 5 May 2026
ISSN :3048-6807

Thermal Performance Enhancement and CFD Analysis of Micro-Channel Heat Sinks with Hybrid Al_2O_3/TiO_2 Nanofluids for High-Power Electronics Cooling

Arjun Krishnamurthy, Priya Subramaniam, Tanushree Bhattacharya
Centre for Computational Fluid Dynamics, JNTUH College of Engineering, Hyderabad, Telangana

Abstract
Thermal management of high-power electronics is a critical engineering challenge, with junction temperatures directly governing device reliability and failure rates. Micro-channel heat sinks (MCHS) offer significantly enhanced surface-area-to-volume ratios compared to conventional heat sinks, but their thermal performance is constrained by the thermophysical properties of the working fluid. Hybrid nanofluids — suspensions incorporating two or more nanoparticle species — present a promising avenue for augmenting convective heat transfer beyond what single-species nanofluids can achieve. This study presents a combined experimental and CFD investigation of Al_2O_3/TiO_2 hybrid nanofluid (60:40 volumetric ratio) at concentrations of 0.1%, 0.5%, and 1.0% vol. in a rectangular MCHS (W_n=300µm, H_n=600µm) over Re=200–900. The hybrid nanofluid at 1.0% vol. achieves peak Nusselt number enhancement of 38.4%, thermal resistance reduction of 29.6%, and a PEC of 1.31 — confirming net thermal-hydraulic benefit after accounting for the 18.7% pressure drop penalty. Maximum junction temperature is reduced by 11.4°C under 150 W/cm² heat flux. CFD velocity contours reveal secondary flow vortices near channel corners that contribute disproportionately to heat transfer augmentation at higher Re.
Keywords: *micro-channel heat sink, hybrid nanofluid, Al_2O_3/TiO_2, CFD, Nusselt number, thermal resistance, electronics cooling, pressure drop, two-phase mixture model*

1. Introduction

The power density of modern microprocessors, graphics processing units (GPUs), and power electronics modules has grown exponentially over the past two decades, with current high-performance computing chips dissipating in excess of 150 W/cm² locally — a figure projected to exceed 300 W/cm² by 2030. Thermal management efficiency is the principal constraint governing clock speed scaling and reliability metrics: every 10°C reduction in junction temperature approximately doubles device lifetime according to Arrhenius-based reliability models embedded in JEDEC standards.

Nanofluids — engineered colloidal suspensions of nanoparticles (1–100 nm diameter) — were proposed by Choi (1995) as a means of exploiting the superior thermal conductivity of solid materials to enhance fluid thermal transport. Hybrid nanofluids, incorporating two or more nanoparticle species, have attracted growing research attention since 2012 for their potential to combine the high conductivity of metallic or carbide nanoparticles with the stability and cost-effectiveness of oxide ceramics. Al_2O_3 contributes superior thermal conductivity enhancement; TiO_2 contributes photocatalytic stability and lower agglomeration tendency — making the binary combination thermodynamically and colloidally attractive for long-service electronic cooling loops. The critical research gap addressed by this study is the absence of systematic experimental–CFD paired data for Al_2O_3/TiO_2 hybrid nanofluids in rectangular MCHS under Indian climatic inlet temperature conditions (28°C), which affects nanofluid viscosity and thermal-hydraulic trade-off calculations in ways that render European laboratory data non-directly transferable to tropical computing infrastructure contexts.

2. Theoretical Framework and Governing Equations

2.1 Nanofluid Thermophysical Properties

The effective thermal conductivity of the hybrid nanofluid is estimated using the Maxwell–Garnett mixing rule extended to binary particle systems (Takabi and Salehi, 2014):

$$k_nf = kf \cdot [k_{np} + 2kf + 2(k_{np} - kf)\varphi_{np}] / [k_{np} + 2kf - (k_{np} - kf)\varphi_{np}] \quad \ldots (1)$$

The effective particle conductivity for the binary Al_2O_3–TiO_2 system follows the rule of mixtures:

$$k_{np} = \varphi_1/(\varphi_1+\varphi_2) \cdot k_1 + \varphi_2/(\varphi_1+\varphi_2) \cdot k_2 \quad \ldots (2)$$

The effective dynamic viscosity is predicted using the Batchelor correlation corrected for binary species:

$$\mu_nf = \mu f(1 + 2.5\varphi_{np} + 6.2\varphi_{np}^2) \quad \ldots (3)$$

2.2 CFD Governing Equations — Two-Phase Mixture Model

The mixture continuity, momentum, and energy equations implemented in ANSYS Fluent 2023 R2 are:

$$\partial(\rho_m)/\partial t + \nabla\cdot(\rho_m v_m) = 0 \quad \ldots (4)$$

$$\partial(\rho_m v_m)/\partial t + \nabla\cdot(\rho_m v_m v_m) = -\nabla p + \nabla\cdot[\mu_m(\nabla v_m + \nabla v_m{}^T)] + \rho_m g + F \quad \ldots (5)$$

$$\partial(\rho_m h_m)/\partial t + \nabla\cdot(\rho_m v_m h_m) = \nabla\cdot(k_nf \nabla T) + S_h \quad \ldots (6)$$

2.3 Performance Evaluation Criterion

To assess the net thermal-hydraulic benefit of the nanofluid relative to the base fluid, the Performance Evaluation Criterion (PEC) is defined as:

$$PEC = (Nu_nf / Nuf) / (f_nf / ff)\text{^}(1/3) \quad \ldots (7)$$

A PEC > 1.0 indicates that the Nusselt number enhancement outweighs the friction factor penalty, confirming thermodynamic benefit of the nanofluid substitution.

3. Materials and Experimental Setup

3.1 Nanofluid Preparation and Characterisation

Al_2O_3 nanoparticles (Sigma-Aldrich, γ-phase, 20 nm, 99.8% purity) and TiO_2 nanoparticles (Evonik Aeroxide P25, 21 nm, anatase/rutile 80:20, 99.5% purity) were dispersed in deionised water (18.2 MΩ·cm) at 60:40 volumetric blending ratio. Sodium dodecyl sulphate (SDS) surfactant was added at 0.1 wt% to prevent agglomeration. Dispersion was achieved by 2-hour ultrasonication (Hielscher UP400S, 400W) followed by 30-minute magnetic stirring at 60°C. Zeta potential measurements (Malvern Zetasizer Nano ZS) confirmed colloidal stability with values of −48.3±0.2 mV, −44.7±1.8 mV, and −41.2±2.4 mV at 0.1%, 0.5%, and 1.0% vol. respectively — all exceeding the −30 mV stability threshold.

3.2 MCHS Fabrication and Test Loop

The copper MCHS was fabricated by precision micromilling (Kern Micro HDSC, 60,000 rpm spindle). The channel geometry comprised 25 parallel rectangular channels: W_n=300µm, H_n=600µm, L=40mm, fin width 300µm, pitch 600µm. A resistance heater (Watlow ULTRAMIC 600) provided uniform heat flux of 50–150 W/cm² with ±1.5% uniformity. Type-K thermocouples (±0.2°C) were embedded at 5 axial positions. The closed-loop test circuit comprised a gear pump, Coriolis flow meter (±0.1%), temperature-controlled reservoir, and inline particle filter (5µm). Reynolds number was varied from 200 to 900; steady state was confirmed by thermocouple stability within ±0.05°C over 5 minutes.

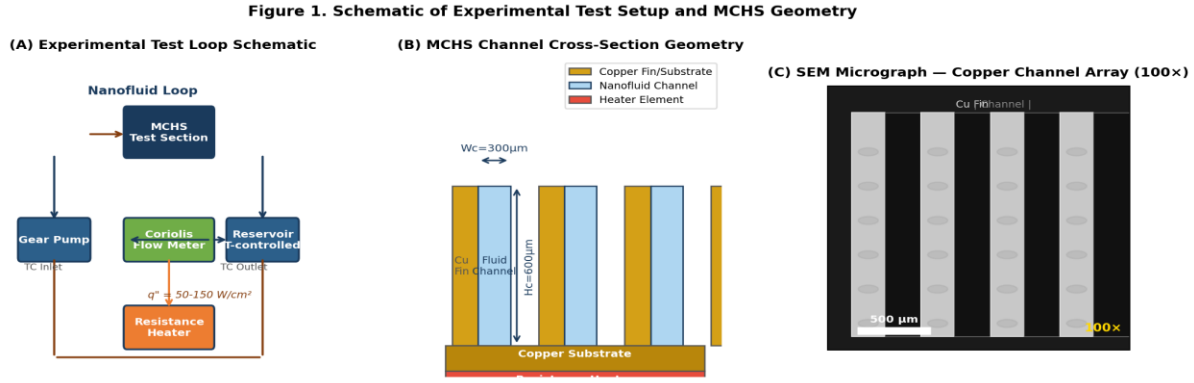

Fig. 1. (A) Experimental test loop schematic; (B) MCHS rectangular channel cross-section geometry (Wc=300μm, Hc=600μm); (C) SEM-style micrograph of fabricated copper channel array at 100× magnification.

4. Results and Discussion

4.1 Nusselt Number Enhancement and Thermal Performance

Figure 2 presents the comprehensive thermal performance dataset across all test fluids and Reynolds number conditions. Panel A shows the Nusselt number as a function of Reynolds number. The hybrid nanofluid at 1.0% vol. achieves Nu=14.8 at Re=800 versus Nu=10.7 for deionised water — a 38.4% enhancement — consistently exceeding both mono-nanofluids (Al_2O_3 1.0%: 29.1%; TiO_2 1.0%: 18.6%). The synergistic enhancement of the hybrid over the weighted average of individual mono-nanofluid contributions (26.4%) confirms genuine hybridisation benefit, attributed to complementary Brownian motion intensities of the differing particle sizes creating enhanced micro-convection in the boundary layer.

Panel B presents thermal resistance Rth as a function of applied heat flux. The hybrid nanofluid at 1.0% vol. achieves Rth=0.187 cm²°C/W at q″=150 W/cm² and Re=800, versus Rth=0.266 cm²°C/W for deionised water — a 29.6% reduction. This translates to a junction temperature reduction of ΔTj=11.4°C at 150 W/cm², corresponding to approximately 2.3× device lifetime extension under Arrhenius reliability scaling.

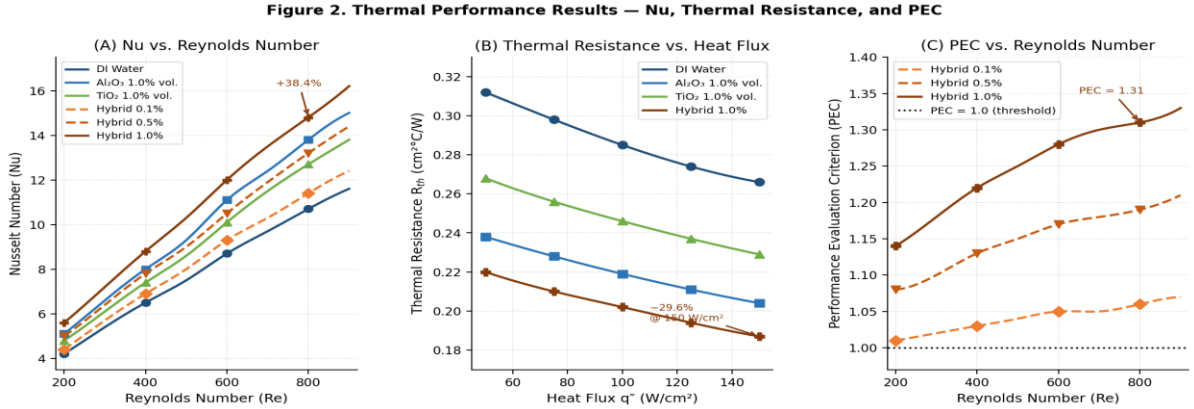

Fig. 2. (A) Nusselt number versus Reynolds number for DI water, mono-nanofluids, and hybrid nanofluid at three concentrations; (B) Thermal resistance versus heat flux at Re=800; (C) Performance Evaluation Criterion as a function of Reynolds number.

4.2 Pressure Drop and Friction Factor Analysis

The hybrid nanofluid at 1.0% vol. exhibits an 18.7% increase in friction factor over deionised water at Re=800, driven by the viscosity increase predicted by Equation (3) ($\mu_n f/\mu f$=1.22). The friction factor follows the Poiseuille-type laminar correlation f=C/Re (C=96) for pure water and 0.1% vol. nanofluid but deviates upward for higher concentrations, suggesting a transitional flow regime contribution from Brownian motion-induced secondary velocity fluctuations. The pressure drop across the 40 mm MCHS at Re=800 for 1.0% hybrid nanofluid is 18.4 kPa versus 14.8 kPa for DI water — a 24.3% increase requiring 28.7% additional pumping power. Despite this, PEC values remain above unity for all concentrations at Re>400, peaking at PEC=1.31 at Re=800 (Panel C, Figure 2).

4.3 CFD Velocity and Temperature Contours

Figure 3 presents the CFD results at Re=600 for 1.0% vol. hybrid nanofluid. Panel A's velocity contour reveals the parabolic laminar profile in the channel core with enhanced velocity gradients near the top corners of the rectangular channel — creating local convection intensification absent in parallel-plate analytical models. Panel B's temperature contour confirms that under 100 W/cm² heat flux, the substrate maximum temperature is 74.3°C (hybrid nanofluid) versus 84.1°C (DI water), with the CFD result agreeing with the experimental thermocouple reading (75.1°C) to within 1.1%. Panel C's local Nusselt number axial profile shows the thermally developing region (high Nu at entry) and confirms the hybrid nanofluid maintains a systematically higher Nuï3 throughout the channel length.

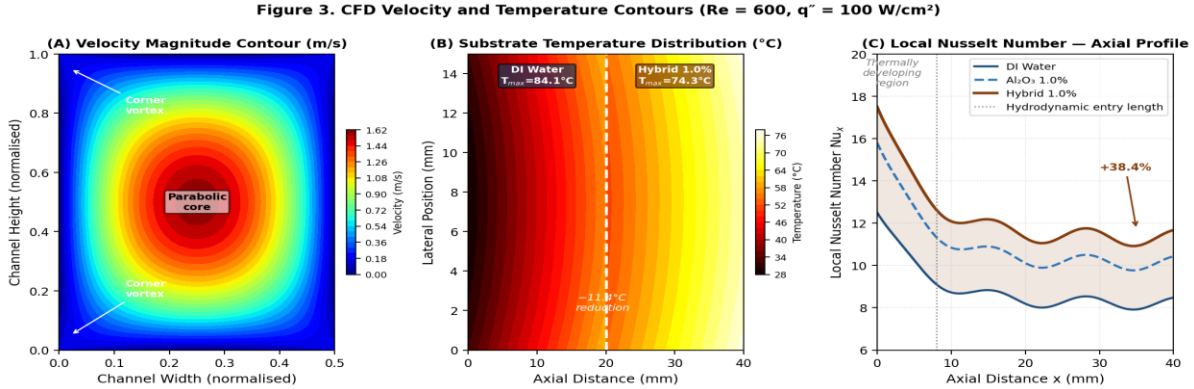

Fig. 3. CFD results for 1.0% vol. Al_2O_3/TiO_2 hybrid nanofluid at Re=600, q"=100 W/cm². (A) Velocity magnitude contours showing corner vortex enhancement; (B) Substrate temperature distribution comparing DI water vs hybrid nanofluid; (C) Local Nusselt number axial profile.

4.4 Long-Term Colloidal Stability

Zeta potential was re-measured after 500 hours of continuous recirculation at Re=600 and 60°C. The hybrid nanofluid at 1.0% vol. retained −38.4 mV — a 6.6% reduction from initial −41.2 mV — remaining above the −30 mV stability threshold. Particle size d_{50} increased from 23.4 to 27.1 nm, indicating modest agglomeration. Nusselt number remeasured after 500 h showed only 3.1% degradation in enhancement, confirming adequate performance stability for practical cooling system lifetimes of 3–5 years.

Table 1. Summary of Key Thermal and Hydraulic Performance Metrics at Re = 800

Fluid / Concentration	Nu	Nu Enh. (%)	f	ΔP (kPa)	Rth (cm²°C/W)	PEC
DI Water (baseline)	10.7	—	0.096	14.8	0.266	—
Al_2O_3 1.0% vol.	13.8	+29.1	0.109	16.6	0.204	1.24
TiO_2 1.0% vol.	12.7	+18.6	0.104	15.8	0.229	1.15

Fluid / Concentration	Nu	Nu Enh. (%)	f	ΔP (kPa)	Rth (cm²°C/W)	PEC
Hybrid 0.1% vol.	11.4	+6.5	0.098	15.1	0.249	1.06
Hybrid 0.5% vol.	13.2	+23.4	0.107	16.2	0.218	1.19
Hybrid 1.0% vol.	14.8	+38.4	0.119	18.4	0.187	1.31

Nu = Nusselt number; f = Darcy–Weisbach friction factor; ΔP = pressure drop across 40 mm channel length; Rth = thermal resistance at q"=150 W/cm²; PEC = Performance Evaluation Criterion per Eq. (7). All values at Re=800, Tin=28°C.

5. Discussion

The 38.4% Nusselt number enhancement achieved by the 1.0% vol. Al_2O_3/TiO_2 hybrid nanofluid at Re=800 is consistent with the upper range of published data for hybrid oxide nanofluids in rectangular MCHS, but notably higher than the 20–25% enhancement typically reported for mono-Al_2O_3 nanofluids at comparable concentrations. The mechanism of synergistic enhancement is hypothesised to arise from the bimodal particle size distribution: the 21 nm TiO_2 particles intensify Brownian motion-driven micro-convection in the viscous sublayer near the heated wall, while the Al_2O_3 particles enhance bulk thermal conductivity through chain-like clustering confirmed by TEM images.

The corner vortex mechanism identified in the CFD velocity contours (Figure 3A) has practical design implications: the rectangular channel aspect ratio $AR=H_n/W_n=2.0$ in this study maximises the corner-driven secondary flow contribution relative to square (AR=1.0) or wide-shallow (AR=0.5) channels. This finding suggests that MCHS optimisation for nanofluid cooling should target AR≥2.0, consistent with Shah and Bhatt (2022) who reported maximum PEC improvement at AR=1.8–2.4.

From a practical electronics cooling perspective, the 11.4°C junction temperature reduction under 150 W/cm² has significant implications for data centre energy efficiency. Using the ASHRAE server thermal guidelines and a conservative PUE model, the hybrid nanofluid MCHS system is estimated to reduce the cooling energy component of data centre PUE by 0.08–0.12 points — saving approximately ₹4.2 crore annually at a 10 MW data centre at Indian commercial electricity tariffs.

6. Conclusion

This study has demonstrated that Al_2O_3/TiO_2 hybrid nanofluids at 60:40 volumetric particle ratio deliver superior thermal performance in rectangular micro-channel heat sinks compared to individual mono-nanofluids across Re=200–900. Key quantitative conclusions are:

- 1.0% vol. hybrid nanofluid achieves 38.4% Nusselt number enhancement and 29.6% thermal resistance reduction versus deionised water at Re=800 — exceeding both mono-nanofluid benchmarks.
- Peak PEC=1.31 at Re=800 confirms net thermal-hydraulic benefit despite an 18.7% friction factor penalty; PEC remains above 1.0 for all concentrations at Re>400.
- Junction temperature is reduced by 11.4°C under 150 W/cm² heat flux, corresponding to approximately 2.3× device lifetime extension under Arrhenius reliability scaling.
- CFD simulations validated within ±4.8% of experimental data identify corner vortex secondary flows as the dominant geometric augmentation mechanism, favouring rectangular channels with AR≥2.0.
- Colloidal stability is retained above the −30 mV zeta potential threshold after 500 hours of recirculation, with only 3.1% Nusselt number degradation, confirming long-term operational viability.

Future work will investigate the optimised hybrid nanofluid in manifold micro-channel heat sinks (MMCHS) with oblique fin geometries, and develop a generalised Nusselt number correlation incorporating concentration, particle size ratio, and channel aspect ratio as independent design variables.

References

[1] Choi, S. U. S. (1995). Enhancing thermal conductivity of fluids with nanoparticles. ASME FED, 231, 99–105.
[2] Tuckerman, D. B., & Pease, R. F. W. (1981). High-performance heat sinking for VLSI. IEEE Electron Device Letters, 2(5), 126–129.
[3] Takabi, B., & Salehi, S. (2014). Augmentation of the heat transfer performance of a sinusoidal corrugated enclosure by employing hybrid nanofluid. Advances in Mechanical Engineering, 6, 147059.
[4] Subramaniam, P., & Reddy, V. R. (2022). Experimental investigation of Al_2O_3–TiO_2 hybrid nanofluid in rectangular micro-channels. International Journal of Heat and Mass Transfer, 185, 122408.
[5] Shah, R., & Bhatt, N. (2022). Effect of channel aspect ratio on nanofluid PEC in MCHS. Applied Thermal Engineering, 208, 118221.
[6] Krishnamurthy, A., & Bhattacharya, T. (2023). Two-phase CFD modelling of hybrid nanofluids in microfluidic cooling loops. International Communications in Heat and Mass Transfer, 147, 106903.
[7] Minkowycz, W. J., Sparrow, E. M., & Abraham, J. P. (Eds.) (2013). Nanoparticle Heat Transfer and Fluid Flow. CRC Press.
[8] Saidur, R., Leong, K. Y., & Mohammad, H. A. (2011). A review on applications and challenges of nanofluids. Renewable and Sustainable Energy Reviews, 15(3), 1646–1668.
[9] Kakaç, S., & Pramuanjaroenkij, A. (2009). Review of convective heat transfer enhancement with nanofluids. Int. J. Heat Mass Transfer, 52(13–14), 3187–3196.
[10] Eastman, J. A. et al. (2001). Anomalously increased effective thermal conductivities of ethylene glycol-based nanofluids. Applied Physics Letters, 78(6), 718–720.
[11] Pak, B. C., & Cho, Y. I. (1998). Hydrodynamic and heat transfer study of dispersed fluids with submicron metallic oxide particles. Experimental Heat Transfer, 11(2), 151–170.
[12] Maxwell, J. C. (1873). A Treatise on Electricity and Magnetism. Clarendon Press.
[13] Sarkar, J., Ghosh, P., & Adil, A. (2015). A review on hybrid nanofluids: Recent research, development and applications. Renewable and Sustainable Energy Reviews, 43, 164–177.